Fragmentation of endohedral fullerene Ho_{3}N@C_{80} in an intense femtosecond near-infrared laser field

Hui Xiong, Li Fang, Timur Osipov, Nora G. Kling, Thomas J. A. Wolf, Emily Sistrunk, Razib Obaid, Markus Gühr, and Nora Berrah

Phys. Rev. A **97**, 023419 — Published 22 February 2018

DOI: 10.1103/PhysRevA.97.023419

Fragmentation of endohedral fullerene $Ho_3N@C_{80}$ in an intense femtosecond near-infrared laser field

Hui Xiong[1], Li Fang[2], Timur Osipov[3], Nora G. Kling[1], Thomas J. A. Wolf [4], Emily Sistrunk [4], Razib Obaid[1], Markus Gühr [4,5], and Nora Berrah [1]

[1]University of Connecticut, Physics Department, Storrs, CT 06269, USA
[2]University of Texas, Center for High Energy Density Science, Austin, TX 78712, USA
[3]LCLS, SLAC National Accelerator Laboratory, Menlo Park, CA 94025, USA
[4]Stanford PULSE Institute, SLAC National Accelerator Laboratory, Menlo Park, CA 94025, USA.
[5]Institut für Physik und Astronomie, Universität Potsdam, 14476 Potsdam, Germany

Abstract:

The fragmentation of gas phase endohedral fullerene, $Ho_3N@C_{80}$, was investigated using femtosecond near-infrared (NIR) laser pulses with an ion velocity map imaging (VMI) spectrometer. We observed that Ho^+ abundance associated with carbon cage opening dominates at an intensity of 1.1×10^{14} W/cm^2. As the intensity increases, the Ho^+ yield associated with multi-fragmentation of the carbon cage exceeds the prominence of Ho^+ associated with the gentler carbon cage opening. Moreover, the power law dependence of Ho^+ on laser intensity indicates that the transition of the most likely fragmentation mechanisms occurs around 2.0×10^{14} W/cm^2.

I. Introduction

Ionization and fragmentation of molecules in femtosecond laser fields is an important method to understand their electronic and nuclear dynamics [1-10]. Complex molecular targets, such as carbon based nano-size fullerenes, characterized by their hollow geometric structures, attract a great deal of interest due to their broad range of applications and 'supramolecular' physical and chemical properties [11]. Fullerenes often exhibit hybrid properties that bridge the gap between small molecules and bulk solids in many aspects [7,12,13].

Based on previous studies on C_{60} ionization and relaxation induced by femtosecond laser pulses, the fragmentation of C_{60} in a strong laser field (~10^{13}-10^{15} W/cm^2) takes place as the following scenario [14,15]: First, the molecule absorbs photons causing both multiple ionization and an increase in the initial internal energy. The photon absorption cross section for C_{60} was estimated to be 0.04 Å^2 (~4 Mbarn) for 800-nm photons, with an uncertainty of a factor of two [16]. Second, the charges and the energy are redistributed within the electronic degrees of freedom via electron-electron coupling on a typical time scale of around 50 fs [14]. At this point, electron-electron scattering may lead to thermal-ionization, elevating the charge state of the C_{60} [16,17]. Third, the energy further redistributes into the nuclear backbone via electron-phonon coupling on a time scale of around a few hundred femtoseconds [18]. These three processes lead to the molecular fragmentation due to the further relaxation of the thermalized molecule as well as the Coulomb energy introduced by multiple ionization [19].

Encapsulation of atoms or molecules by the carbon cage alters the electronic properties of pure carbon fullerenes [8,20,21], and the behavior of endohedral fullerenes in a strong laser field can be very different from that of empty fullerenes. For instance, an encaged planar Ho_3N moiety in C_{80} breaks the symmetry of C_{80} and makes the super-atomic molecular orbital (SAMO) states optically accessible [8]. The understanding of the ionization and fragmentation of endohedral fullerenes is not as comprehensive as for C_{60}, due to extra theoretical and experimental complications. Nevertheless, a few studies regarding the fragmentation dynamics in endohedral fullerenes have been carried out, focusing on neutral carbon dimer emission induced by single X-ray photons or single pulse optical lasers [22-25], or the formation of new chemical bonds between atoms from the cage and the enclosed species [9,26-28]. Recently, we found that the endohedral fullerene's internal energy plays an important role in the fragmentation of X-ray excited $Sc_3N@C_{80}$ [29]. In addition, three significant fragmentation processes were identified: 1) evaporation of C_2, 2) emission of small molecular carbon ions (C_n^+, $n \leq 24$), and 3) release of Sc and Sc-containing ions associated with carbon cage opening or fragmentation [29].

In this work, we studied the fragmentation of gas phase endohedral fullerene $Ho_3N@C_{80}$ using a strong 800 nm laser field. $Ho_3N@C_{80}$ is a trimetallic nitride templated endohedral metallofullerene (TNT-EMFs), one of the most widely synthesized types of endohedral fullerenes. To avoid the complexity due to several absorption and relaxation mechanisms, we employed laser pulses with 30 fs pulse duration, which is about the time scale of electron-electron coupling (50 fs) and shorter than electron-phonon coupling [14]. We identified three different main fragmentation processes: 1) removal of an even number carbon atoms, 2) emission of atomic and molecular carbon ions, and 3) release of Ho and Ho-containing ions associated with the carbon cage opening or multi-fragmentation of the C_{80} carbon cage. The kinetic energy distribution (KED) of Ho^+ indicated that the fullerene's fragmentation mechanism changes from cage opening to cage multi-fragmentation with increasing laser intensity.

II. Experimental setup

The experiment was performed using a coincidence scheme with a VMI spectrometer. Details of the spectrometer have been thoroughly described in previous work [8,30,31]. Briefly, a static electric field applied across the interaction region served to extract electrons and ions from the interaction region. The extracted ions were guided through a set of electrodes in VMI configuration and a 50-cm-long drift tube, and were detected by a multi-hit-capable time and position-sensitive detector (RoentDek). The time of flight for the ions as well as their positions on the detector were measured, and were used to reconstruct their three-dimensional (3D) momenta and kinetic energies (KEs).

The $Ho_3N@C_{80}$ sample was obtained from SES Research and has a purity of 95%. According to SES Research, the impurities are mainly TNT-EMFs with bigger carbon cages than $Ho_3N@C_{80}$, i.e. $Ho_3N@C_{82, (84, 86)}$, as well as a small amount of endohedral fullerene with a smaller carbon cage. Less than 0.1% of the impurity is attributed to unfilled fullerenes. The gas phase sample was obtained by evaporative heating in an 800 K oven, mounted on a 3-dimensional translation stage at the top of the chamber. The evaporated molecules were introduced into the vacuum chamber through a nozzle and a skimmer with a 1 mm aperture. Prior to the experiment, the

sample was heated up to about 400 K for ~12 hours to evaporate any residual solvent molecules. For the duration of the experiment, the background pressure inside the chamber was kept below 3×10^{-8} mbar. The VMI spectrometer was perpendicular to the axis of the oven.

The laser pulses intersected the $Ho_3N@C_{80}$ molecular beam at the center of the vacuum chamber, between the repeller and extractor plates of the VMI spectrometer. The ultrashort laser pulses were delivered by a commercially available Ti:Sapphire laser system. The measured pulse duration and central wavelength were 30 fs and 800 nm, respectively. The peak laser intensity was varied by an attenuator consisting of a half waveplate and two thin-film polarizers by two orders of magnitude (10^{13} – 10^{15} W/cm^2). The polarization of the laser field at the interaction region was horizontal, i.e. along the axis of the VMI spectrometer. The laser was focused at the center of the extraction zone by a lens with 35 cm focal length. The laser intensity was calibrated by measuring the ionization yield of Ar as a function of laser power, and following the procedure proposed by Hankin *et al.* [32].

III. Experimental Results and Discussion

a) Assignment of the observed ions

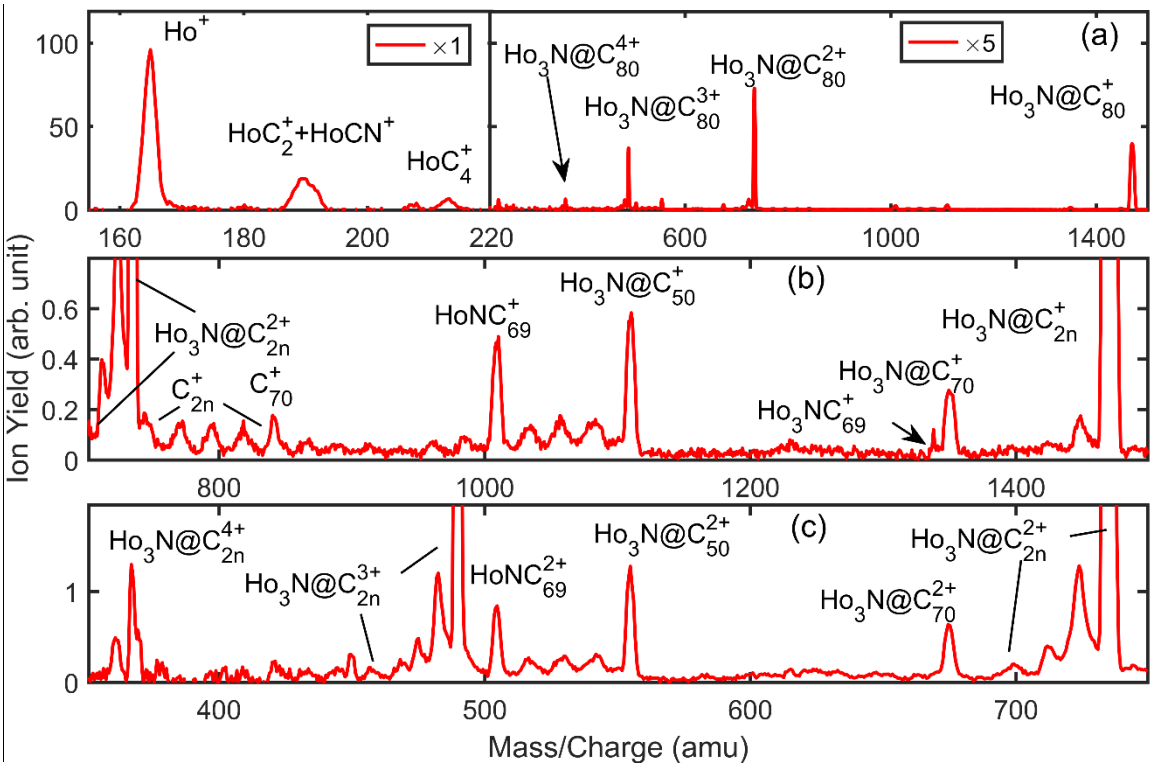

Figure 1. (Color online) Mass/charge (m/q) spectra of $Ho_3N@C_{80}$ at a laser intensity of 4×10^{14} W/cm^2. (a) Overall m/q spectrum. The spectrum for m/q > 220 has been multiplied by 5. (b) Zoomed-in spectrum displaying peaks between the singly and doubly charged parent ions. In this panel, $38\le n\le40$ for $Ho_3N@C_{2n}^+$, $37\le n\le40$ for $Ho_3N@C_{2n}^{2+}$, and $31\le n\le37$ for C_{2n}^+. (c) Spectrum displaying peaks between the doubly and quadruply charged parent ions. In this panel, $37\le n\le40$ for $Ho_3N@C_{2n}^{2+}$, $36\le n\le40$ for $Ho_3N@C_{2n}^{3+}$, and $39\le n\le40$ $Ho_3N@C_{2n}^{4+}$. Note that the detection efficiency of the detector is not taken into account.

A typical m/q spectrum of $Ho_3N@C_{80}$ exposed to a strong laser field is shown in Fig. 1. The left panel of Fig. 1(a) shows Ho-containing molecular ion fragments, including HoC_2^+, $HoCN^+$, HoC_4^+, as well as atomic Ho^+. The right panel Fig. 1(a) shows mainly multiply-charged parent molecular ions, up to the quadruply charged state. The spectrum in the region between the singly and doubly charged parent molecules is shown in Fig. 1(b). Fullerenes that have lost an even number of carbon atoms are identified as $Ho_3N@C_{78}^+$, $Ho_3N@C_{76}^+$, $Ho_3N@C_{70}^+$ and $Ho_3N@C_{50}^+$. This observed loss of an even number of carbon atoms was also observed for C_{60}, and other endohedral fullerenes subjected to laser fields [27,33,34], or X-rays [9,10]. An interesting observation is that the abundance of $Ho_3N@C_{70}^+$ and $Ho_3N@C_{50}^+$, where a large part of the cage has disappeared, is significantly higher than singly charged fragments, such as $Ho_3N@C_{2n}^+$ (2n=78 and 76), where only small pieces of the cage are missing. The abnormally large $Ho_3N@C_{70}^+$ and $Ho_3N@C_{50}^+$ yields observed might be due to the release of even numbers of carbon atoms simultaneously instead of sequential release of C_2. This latter process is the most significant fragmentation pathway of removing small even number (2n, n≥2) of carbon atoms from a charged C_{60} [35,36].

Two peaks corresponding to the loss of an odd number of carbons, $Ho_3NC_{69}^+$ and $HoNC_{69}^+$, were also observed. Additionally, the small peaks between 948 amu and 1093 amu are likely fullerenes that released two Ho along with some C and N ions ($HoNC_{2n-1}^+$ and HoC_{2n}, $66<2n<76$). Due to the isotopes of carbon and nitrogen, along with the peak broadening owing to recoil, we unfortunately were not able to distinguish fullerene ions, $HoNC_{2n-1}^+$ and HoC_{2n}. For fullerene ions, $Ho_3NC_{69}^+$, $HoNC_{69}^+$, and $HoNC_{2n-1}^+$, the cage may have the form of an azafullerene, such as $C_{69}N$ [37]. Fullerenes with all three Ho atoms released are observed around 800 amu. Similarly, we were not able to distinguish if those peaks are C_{2n}^+ or $C_{2n-1}N^+$ ($62<2n<74$) in the spectrum. For comparison, the x-axis in Fig. 1(c) is set to align the doubly charged fragments with the same mass as the singly charged fragments in panel (b). Here, we clearly see a correlation between the singly and doubly charged ions.

b) Identification of the $Ho_3N@C_{80}$ fragmentation pathways associated with Ho^+

To identify the fragmentation pathways of complex molecules, ion-ion coincidence mapping, which connects different fragments from single dissociation events, is widely used [38]. However, in experiments where intense lasers are employed, many ions and electrons can be created from multiple targets in a single shot, leading to false coincidences. A good alternative to coincidence mapping is covariance mapping, which is employed particularly in experiments where many ions or electrons are generated per laser shot [39-41]. We integrated the covariance signal associated with Ho^+, and show it in Fig. 2. We emphasize that, although Fig. 2(a) shows reasonably clean peaks, this analysis may not be used as a quantitative measure of the fragment yield.

In general, it is clear from the covariance with Ho^+ that multiple fragmentation occurs for both the cage and the encapsulated species. While C^+ is observed, there is no sign of multiply charged atomic carbon ions. Molecular carbon fragment ions from C_2^+ up to C_{23}^+ are also observed, as shown in Fig. 2(a) and 2(b). Similar patterns with small molecular carbon fragment ions have been observed previously in experiments on C_{60} and $Ho_3N@_{80}$ using high excitation energy [9,42]. To generate small molecular carbon ions from the fragmentation of C_{60} and C_{60}^+, Campbell *et al.* established with a simple statistical theory that an average internal energy of 100 eV is needed

[43]. In addition to the statistical behavior, a pump-probe experiment also indicates that small carbon fragments may also arise from direct fragmentation (as opposed to statistical behavior) on a picosecond time-scale at an intensity as low as a few 10^{13} W/cm^2 [44]. This direct fragmentation does not affect the discussion in this report since only the post-ionization or dissociative ionization processes induced by the probe pulse can lead to significant increase on the yield of atomic or molecular carbon ions. Since the encapsulation of moieties has little impact on how C-C bonds breaks up, we assume here that high internal energy is also required to create small molecular carbon ions from $Ho_3N@C_{80}$. Other Ho-containing molecular ions, such as $HoCN^+$ and Ho combined with an even number of carbon atoms up to HoC_8^+ are observed in Fig. 2(a) and (b). The $HoCN^+$ and some of the Ho carbide ions were also observed when $Ho_3N@C_{80}$ was exposed to a strong X-ray free electron laser [9]. We note that although Ho donates three charges to its environment, the predominant charge state measured for Ho and Ho-containing fragments are singly charged. Thus one can make a simple assumption that, during the early dissociation stages, the electrons are captured at the Ho sites [9].

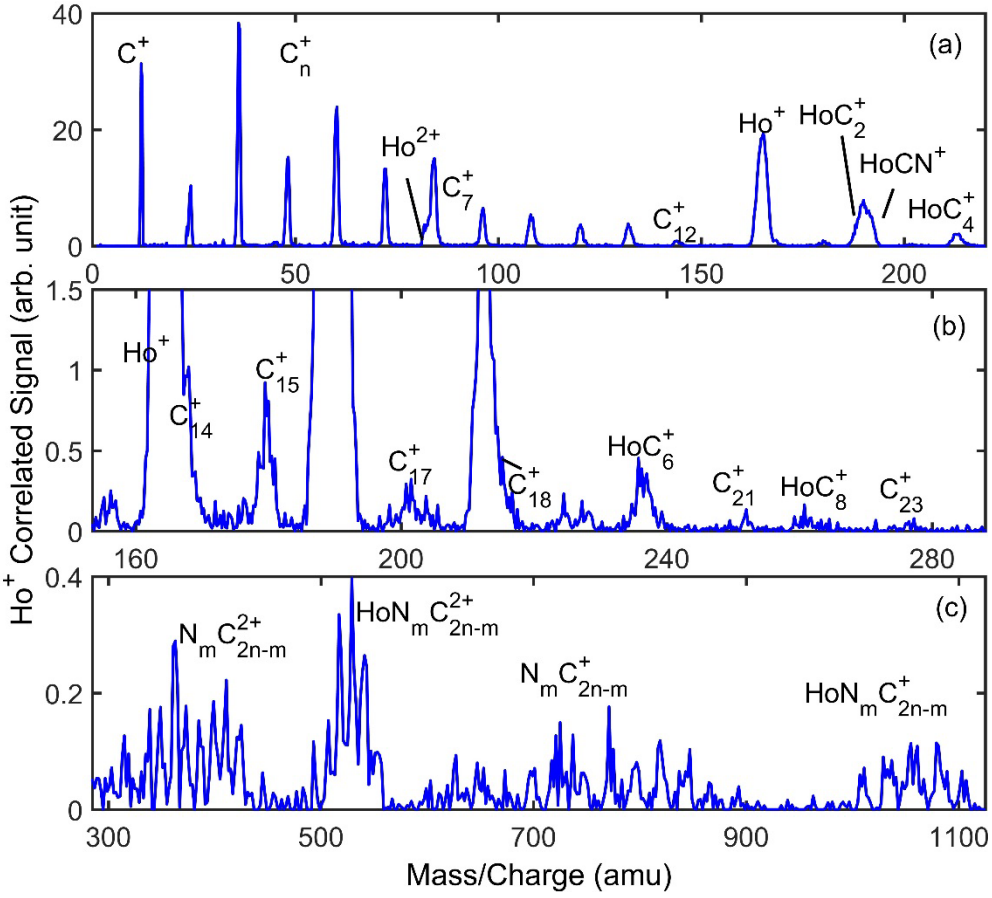

Figure 2. (Color online) Fragment ions correlated with Ho^+ from $Ho_3N@C_{80}$ molecules produced in a 4×10^{14} W/cm^2 laser field using the covariance mapping technique. (a) Spectrum showing low m/q range for atomic and molecular carbon ions, Ho^+, and Ho-containing ions. (b) Spectrum showing mid m/q for heavy molecular carbon ion fragments and Ho-containing ion fragments. (c) Spectrum showing high m/q for the heavy fullerene ion fragments, $N_mC_{2n-m}^+$ ($58\le2n\le74$), $N_mC_{2n-m}^{2+}$ ($52\le2n\le70$), $HoN_mC_{2n-m}^+$ ($70\le2n\le78$), and $HoN_mC_{2n-m}^{2+}$ ($68\le2n\le78$), with $m= 0,1$.

Fig. 2(c) shows the heavier fullerene fragment ions, *i.e.* $N_mC_{2n-m}^+$ ($58\leq 2n\leq 74$), $N_mC_{2n-m}^{2+}$ ($52\leq 2n\leq 70$), $HoN_mC_{2n-m}^+$ ($70\leq 2n\leq 78$), and $HoN_mC_{2n-m}^{2+}$ ($68\leq 2n\leq 78$), with m= 0,1. Here we list m=0 or 1 because we are not able to distinguish the difference of 2 amu on these peaks due to the broadening by recoil as well as the presence of C and N isotopes. The peak identified as $HoNC_{69}^+$ is also suppressed compared to the raw m/q spectrum (see Fig. 1(b, c)), suggesting that $HoNC_{69}$ was an impurity (less than 0.1% according to SES Research). A few sets of fragments can be identified in this spectrum. One set of fragments is located at m/q from 1007 to 1104 amu, corresponding to the fragmentation processes that release 2 Ho and an odd number of C or N atoms. The right most peak in this set is at ~1104 amu, corresponding to a release of two Ho and three C and/or N atoms ($HoN_mC_{78-m}^+$, m=0,1), either the combination of two C and one N, or three C atoms. The left most peak in this series at ~1007 amu corresponds to a removal of 2 Ho and 11 C and/or N atoms ($HoN_mC_{70-m}^+$, m=0,1). The second set of fragments, found between 624 and 891 amu, are those where roughly half of the cage remains intact and forms a bond to the N atom, while all three Ho atoms have dissociated from the system ($N_mC_{2n-m}^+$, $58\leq 2n\leq 74$). These two sets of fragments have similar characteristics in both the singly and doubly charged states. No evidence of endohedral fullerene fragments with the two remaining Ho still encaged was found associated with Ho^+. Fullerenes containing 2 Ho might not be able to retain thermal equilibrium without further fragmentation due to the enormous energy deposited into the system by the strong laser field.

With the covariance map technique, we identified two predominant processes that are associated with the release of Ho^+. One process is multiple fragmentation of the cage into many atomic and small molecular carbon ions C_n^+ ($1<n<23$). As a result, the Ho^+ is exposed by the shattered carbon cage. The other process is the emission of Ho^+ from the parent or intermediate endohedral fullerenes, likely through Coulomb repulsion between Ho^+ and the rest of the fullerene, i.e., Ho^+ escapes from the nearly intact carbon cage. In the latter case, at least a temporary opening on the carbon cage is needed for the Ho to escape. Our current understanding suggests a mechanism based on temporary bond breaking without fragmentation as explained in the following. Many photons can be absorbed by a fullerene molecule in the strong laser field before fragmentation. For instance, a few tens of photons could be absorbed by a C_{60} molecule at a laser intensity of 1×10^{14} W/cm^2 in an 800-nm laser field. Due to the large amount of energy deposited into the fullerene by the strong laser field, the carbon backbone becomes highly thermalized and a great number of bonds between two neighboring C atoms may be temporarily broken without fully fragmenting from the system, or simply allow 'cage opening' [45-47]. Indeed, Laarmann *et al.* demonstrated that a few tens of 800 nm photons can be absorbed at laser intensity ~10^{14} W/cm^2, leading to a large amount of deposited energy and temporarily broken (elongated) bonds of neighboring carbon atoms allowing for cage opening [48].

c) KED of Ho^+

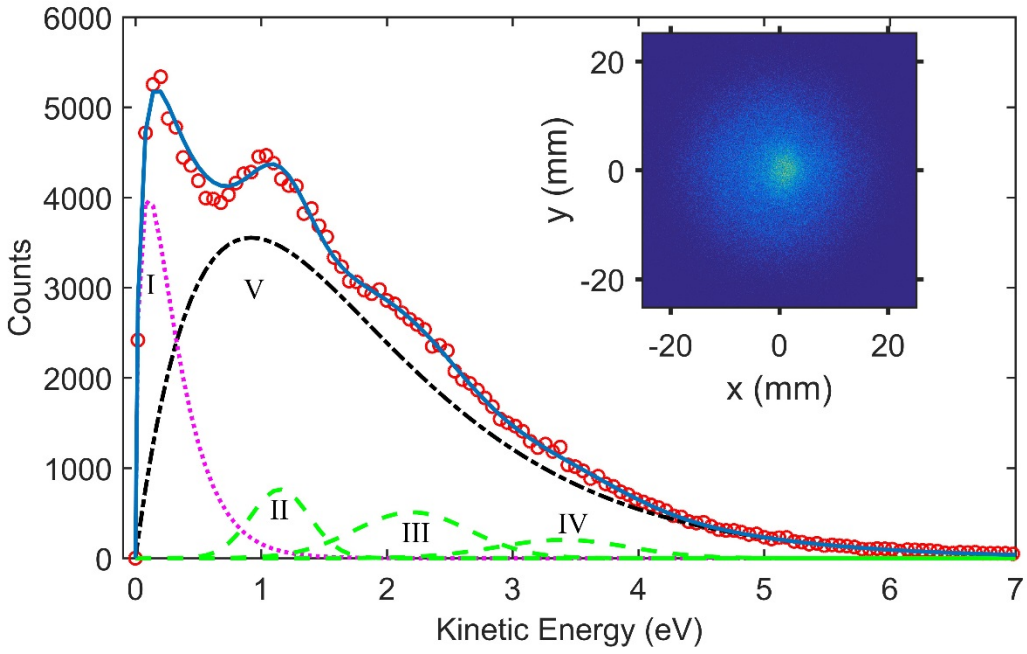

Figure 3. (Color online) KED of Ho^+ from $Ho_3N@C_{80}$ at the laser intensity of 4×10^{14} W/cm^2. The red circles and solid blue line are the experimental KE spectrum and its fitted curve, respectively. The fitted spectrum consists of three components: 1) Ho^+ emission through Coulomb repulsion associated with carbon cage opening (three green dashed line), 2) Ho^+ emission through escaping associated with cage opening (magenta dotted line) and 3) Ho^+ emission associated with carbon cage multi-fragmentation (black dash dotted line). The inset shows the VMI image of Ho^+.

To understand the fragmentation dynamics, we examine the kinetic energy (KE) of Ho^+, as shown in Fig. 3. The tail of the overall KED curve is fitted by the "model-free" method by Klots [49], which has been used extensively in other previous work [23,50-55] (dash-dotted curve in Fig. 3, labeled V),

$$P(\epsilon) = a\epsilon^{l}\exp\left(-l\frac{\epsilon}{\tilde{\epsilon}}\right) \qquad (1)$$

where a is a normalization factor, $\tilde{\epsilon}$ is the position of the maximum of the KE distribution (i.e., the most probable KE value), and l is a parameter related to the interaction potential between the fragments ($0< l <1$). For the best fit, l is found to be close to 1. The rest of the signal was fitted with 4 peaks. The three almost linearly spaced peaks at 1.2, 2.2, and 3.4 eV (labeled as II, III, IV) were fitted with Gaussian distributions. These almost equally-spaced peaks can be explained by Coulomb repulsion, where the fullerene cage opens such that Ho^+ are emitted. For instance, peak II originates from intermediate or parent endohedral fullerenes with 2 charges, emitting a Ho^+ ion while leaving a singly charged fullerene. Similar scenarios happen to peak III and IV, except with parent fullerenes with 3 and 4 charges, respectively. Interestingly, a KE of 1.2 eV corresponds to ~50% of the KE a Ho^+ would share if the Coulomb explosion happens between a Ho^+ and a C_{80}^+ cage. Similar energy loss was also observed in the fragmentation of multiply-charged fullerene dimers [52,56,57], during which half of the Coulomb energy was deposited into the internal energy of the two smaller fullerene fragments. The low energy peak, labeled I, is also fitted with

the model-free method, and *l* for this peak was found to be close to 1 as well. This peak likely manifests from the Ho^+ being emitted from a singly charged parent or intermediate endohedral fullerene during the cage opening, taking away the only charge. As for peak V, the broadened distribution may be explained by Ho^+ being emitted through multi-fragmentation.

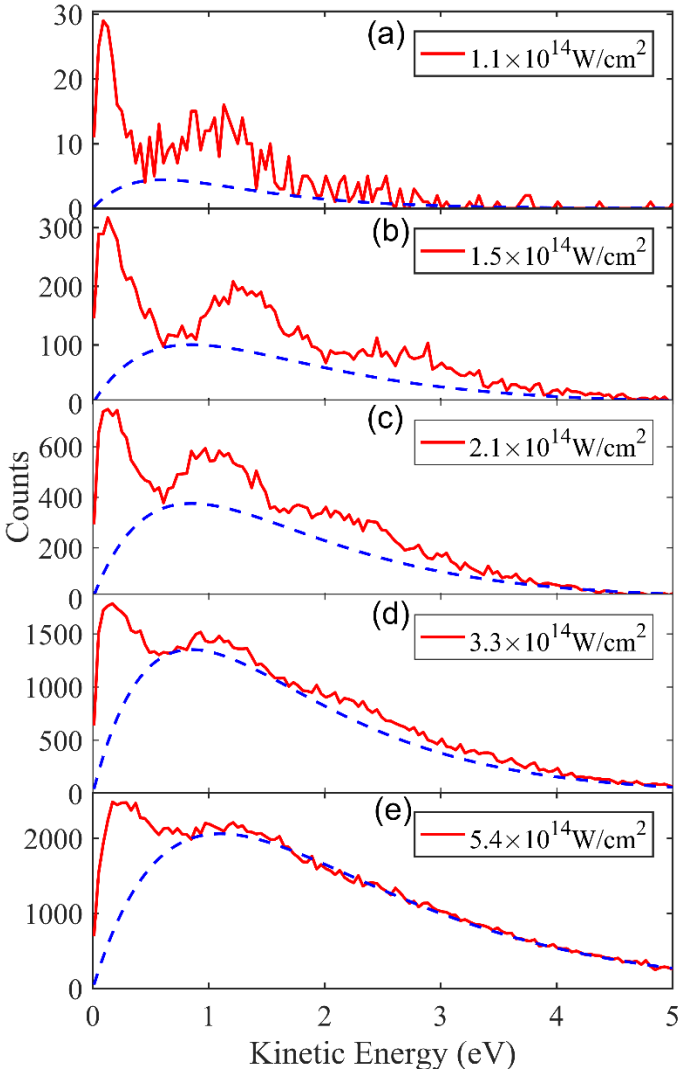

Figure 4. (Color online) KED of Ho^+ at different laser intensities (a) 1.1×10^{14} W/cm^2, (b) 1.5×10^{14} W/cm^2, (c) 2.1×10^{14} W/cm^2, (d) 3.3×10^{14} W/cm^2, and (e) 5.4×10^{14} W/cm^2. The blue dashed lines are the fit for peak V.

Since several laser intensities were used to excite the parent molecules, we were able to study the fragmentation of parent molecules with different internal energies. The KEDs of Ho^+ at five different laser intensities is shown in Fig. 4. When the laser intensity is at 1.1×10^{14} W/cm^2, 1.5×10^{14} W/cm^2, and 2.1×10^{14} W/cm^2, peak I and II are clearly visible. Meanwhile at much higher intensity, such as 5.4×10^{14} W/cm^2, almost all the peaks are nearly indistinguishable. Peak V, which is associated with multi-fragmentation of the cage accounts for 31%, 49%, 63%, 80%, and 87% of the total Ho^+ yield at laser intensity 1.1×10^{14} W/cm^2, 1.5×10^{14} W/cm^2, 2.1×10^{14} W/cm^2,

3.3×10^{14} W/cm^2 and 5.4×10^{14} W/cm^2, respectively, indicating that multi-fragmentation of the cage is the dominant mechanism for Ho^+ emission at intensities higher than 2.0×10^{14} W/cm^2.

Campbell *et al.*[43] argued that a transition to a 'pretzel' phase [47] takes place at internal energy [E] ~80-225 eV for C_{60}, and the fragment's size shifts from being entirely fullerenes ([E] < 80 eV) to entirely small fragments ([E] > 225 eV). We estimate the energy absorbed by $Ho_3N@C_{80}$ using the cross section 0.04 Å^2 of C_{60} in a laser field with intensity 2.0×10^{14} W/cm^2 to be ~120±60 eV (the uncertainty is estimated from the cross-section measurement in [16]). This absorbed energy is not exactly the internal energy since the energy needed for the photoionization of the parent molecule, and the few eV of the initial internal energy [58,59], are not taken into account. However, our estimated absorbed energy qualitatively aligns with the transition internal energy onset of the phase transition [E]=80 eV in C_{60}. This phase transition of the endohedral fullerene can explain the results of Ho^+ associated with cage multi-fragmentation, dominating at laser intensities >2.0×10^{14} W/cm^2.

d) Ho^+ power law

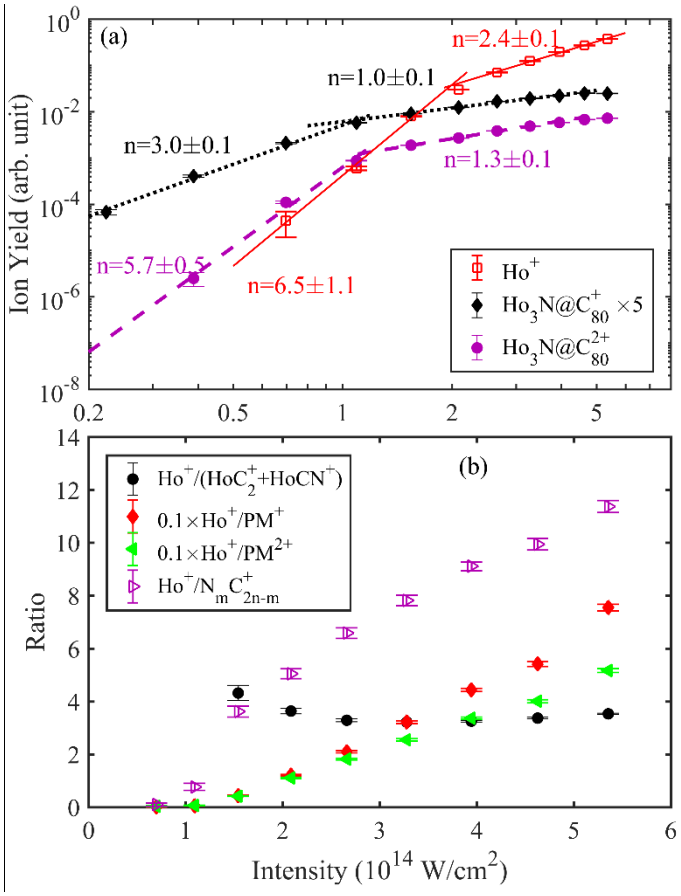

Figure 5. (Color online) (a) The yield of Ho^+ along with the singly, and doubly charged parent molecule (PM) $Ho_3N@C_{80}$, as a function of laser intensity. (b) Branching ratios between the ion yields of Ho^+ and the sum of HoC_2^+ and $HoCN^+$ (black circles), Ho^+ and PM^+ (red diamonds), Ho^+ and PM^{2+}, (green filled triangles), and between Ho^+ and $N_mC_{2n-m}^+$ (64<2n<72, m=0,1) (purple unfilled triangle). The results for the parent molecular ions are reproduced from [8].

The power law, i.e., ion yield as a function of intensity, can help reveal various molecular dynamics processes [8,14,60,61]. The power law for Ho^+ is plotted in Fig. 5(a). The Ho^+ yield increases rapidly with intensity and follows the typical power law I^n, where n=6.5±1.1, and it reduces to n=2.4±0.1 when the laser intensity is higher than the 2.0×10^{14} W/cm^2. The yields of parent molecular ions reproduced from [8] are also shown for comparison. The power law slope for Ho^+ at low intensity is close to that for the doubly charged parent molecule (n=5.7±0.5), suggesting that multiply charged (≥2) parent molecules might be the predominant source for Ho^+ production. The yields of parent molecular ions also have similar two-slope features. The intensity at the crossing point of the two slopes is defined as the saturation intensity [33], and the slope (1<n<1.5) beyond the saturation point is caused by the so-called volume effect due to a non-uniform laser intensity at the focal spot [32]. However, the slope for Ho^+ at intensity higher than 2.0×10^{14} W/cm^2 is steeper than the n=1~1.5 slope caused by the saturation ionization. As mentioned earlier, the fragmentation of fullerenes depends on the energy absorbed from the laser field. The ionization saturation of the parent molecule does not necessarily mean that the energy absorption has saturated. Therefore, a steeper n=2.4±0.1 slope on Ho^+ yield emerges at intensity >2.0×10^{14} W/cm^2. The transition on Ho^+ yield power law at 2.0×10^{14} W/cm^2 also aligns with our finding that multi-fragmentation of the cage is the dominate mechanism for Ho^+ emission at higher intensities (see Fig. 4). Therefore, the transition of the Ho^+ yield power law may originate from the following scenarios: 1) at lower intensities, the internal energy promotes temporary C-C bond breakings, through which Ho^+ may breach out of the open cage, and its yield mainly depends on the yield of the parent molecular ions; 2) at intensities higher than 2.0×10^{14} W/cm^2, high internal energy makes cage multi-fragmentation the dominant fragmentation process for Ho^+ yield, which may reflect on the energy absorbed by the carbon cage.

Fig. 5(b) shows the branching ratios between Ho^+ and the parent molecular ions, $N_mC_{2n-m}^+$ and to the sum of HoC_2^+ and $HoCN^+$. The ratios for Ho^+/PM^+ and Ho^+/PM^{2+} increase almost linearly with respect to the laser intensity >1.0×10^{14} W/cm^2, while the branching ratio for $Ho^+/(HoC_2^+ + HoCN^+)$ initially decreases, and then is almost constant above ~2.5×10^{14} W/cm^2. The ratio $Ho^+/N_mC_{2n-m}^+$ increases with the laser intensity. This is because, while the Ho^+ emission mechanism transits into multiple fragmentation for higher laser intensity, the abundance of ion fragments associated with cage opening including $N_mC_{2n-m}^+$ decreases, resulting in a monotonic increase in the branching ratio of $Ho^+/N_mC_{2n-m}^+$.

The ratios between Ho^+ and the parent molecular ions, $Ho^+/N_mC_{2n-m}^+$ are boosted around 1.0×10^{14} W/cm^2 laser intensity, where the saturation of singly and doubly charged parent molecular ions occurs while the absorbed energy still increases with laser intensity. The simple relation between Ho^+ and the parent molecular ions (see Fig. 5(b)) suggest a critical role played by the absorbed energy in the fragmentation of $Ho_3N@C_{80}$ in a femtosecond laser field. Since the laser pulse duration is similar to the time-scale for electron-electron interactions and much shorter than electron-phonon couplings [14], the electronic subsystem of the fullerene is heated up during the laser pulse, while the molecular backbone is still vibrationally cold. i.e. the fragmentation process is the result of the redistribution of the internal energy from the electronic subsystem and the Coulomb energy. This work complements the ionization, fragmentation and ion production of $Ho_3N@C_{80}$ in a femtosecond X-ray laser field [9] as well as X-ray synchrotron-based photoionization work on $Sc_3N@C_{80}$ [29]

IV. Conclusion

We investigated the fragmentation of $Ho_3N@C_{80}$ induced by femtosecond, intense, near-infrared laser pulses. Three different fragmentation processes were identified: the removal of an even number of carbon atoms, the emission of atomic and small molecular carbon ions, and the release of Ho^+ and Ho containing molecular ions via carbon cage opening or cage multiple fragmentation. The KED of Ho^+ at different laser intensities suggests a transition in the mechanisms associated with the production of Ho^+, as well as their emission through cage opening and cage multiple fragmentation. Both the evolution of the KED of Ho^+ at different laser intensities and the almost linear dependence of the ratio between Ho^+ and the parent molecule on laser intensities suggests that the internal energy plays a critical role in the fragmentation of $Ho_3N@C_{80}$ in strong femtosecond laser field.

This work was funded by the Department of Energy, Office of Science, Basic Energy Sciences (BES), Division of Chemical Sciences, Geosciences, and Biosciences under grants Nos. DE-SC0012376 (UConn group). L.F. acknowledges the support by Defense Advanced Research Project Agency Contract 12-63-PULSE-FP014, and by National Nuclear Security Administration Cooperative Agreement DE-NA0002008. M.G. acknowledges funding via the Office of Science Early Career Research Program through the Office of Basic Energy Sciences, U.S. Department of Energy. T.J.A.W. thanks the German National Academy of Sciences Leopoldina for a fellowship (Grant No. LPDS2013-14). We would also like to thank A-M Carroll for assistance with this manuscript.

[1] M. Lezius, V. V. Blanchet, D. M. Rayner, D. M. Villeneuve, A. Stolow, and M. Y. Ivanov, Phys. Rev. Lett. **86**, 51 (2001).
[2] T. Brabec, *Strong Field Laser Physics* (Springer, 2009).
[3] P. Agostini and L. F. DiMauro, Adv. At. Mol. Opt. Phys. **61**, 117 (2012).
[4] C. I. Blaga, J. Xu, A. D. DiChiara, E. Sistrunk, K. Zhang, P. Agostini, T. A. Miller, L. F. DiMauro, and C. D. Lin, Nature **483**, 194 (2012).
[5] E. Goulielmakis, Z.-H. Loh, A. Wirth, R. Santra, N. Rohringer, V. S. Yakovlev, S. Zherebtsov, T. Pfeifer, A. M. Azzeer, M. F. Kling *et al.*, Nature **466**, 739 (2010).
[6] H. Li, B. Mignolet, G. Wachter, S. Skruszewicz, S. Zherebtsov, F. Süßmann, A. Kessel, S. A. Trushin, N. G. Kling, M. Kübel *et al.*, Phys. Rev. Lett. **114**, 123004 (2015).
[7] H. Li, B. Mignolet, Z. Wang, K. J. Betsch, K. D. Carnes, I. Ben-Itzhak, C. L. Cocke, F. Remacle, and M. F. Kling, J. Phys. Chem. Lett **7**, 4677 (2016).
[8] H. Xiong, B. Mignolet, L. Fang, T. Osipov, T. J. A. Wolf, E. Sistrunk, M. Gühr, F. Remacle, and N. Berrah, Sci. Rep. **7**, 121 (2017).
[9] N. Berrah, B. Murphy, H. Xiong, L. Fang, T. Osipov, E. Kukk, M. Guehr, R. Feifel, V. S. Petrovic, K. R. Ferguson *et al.*, J. Mod. Opt. **63**, 390 (2016).
[10] B. F. Murphy, T. Osipov, Z. Jurek, L. Fang, S. K. Son, M. Mucke, J. H. Eland, V. Zhaunerchyk, R. Feifel, L. Avaldi *et al.*, Nat. Commun. **5**, 4281 (2014).
[11] R. Marega, D. Giust, A. Kremer, and D. Bonifazi, in *Supramolecular Chemistry of Fullerenes and Carbon Nanotubes* (Wiley-VCH Verlag, Berlin, 2012), pp. 301.
[12] H. Zettergren, N. Haag, and H. Cederquist, in *Handbook of Nanophysics* (CRC Press, Boca Raton, 2010), pp. 1.
[13] T. Fennel, K. H. Meiwes-Broer, J. Tiggesbäumker, P. G. Reinhard, P. M. Dinh, and E. Suraud, Rev.Mod.Phys **82**, 1793 (2010).

[14] I. Shchatsinin, T. Laarmann, G. Stibenz, G. Steinmeyer, A. Stalmashonak, N. Zhavoronkov, C. P. Schulz, and I. V. Hertel, J. Chem. Phys. **125**, 194320 (2006).
[15] I. Shchatsinin, T. Laarmann, N. Zhavoronkov, C. P. Schulz, and I. V. Hertel, J. Chem. Phys. **129**, 204308 (2008).
[16] K. Hansen, K. Hoffmann, and E. E. B. Campbell, J. Chem. Phys. **119**, 2513 (2003).
[17] E. E. Campbell, K. Hansen, K. Hoffmann, G. Korn, M. Tchaplyguine, M. Wittmann, and I. V. Hertel, Phys. Rev. Lett. **84**, 2128 (2000).
[18] J. R. Verlet, Chem. Soc. Rev. **37**, 505 (2008).
[19] S. Díaz-Tendero, M. Alcamí, and F. Martín, Phys. Rev. Lett. **95**, 013401 (2005).
[20] L. Dunsch and S. Yang, Phys. Chem. Chem. Phys. **9**, 3067 (2007).
[21] A. A. Popov, S. Yang, and L. Dunsch, Chem. Rev. **113**, 5989 (2013).
[22] D. C. Lorents, D. H. Yu, C. Brink, N. Jensen, and P. Hvelplund, Chem. Phys. Lett. **236**, 141 (1995).
[23] J. Laskin, H. A. Jimenez-Vazquez, R. Shimshi, M. Saunders, M. S. de Vries, and C. Lifshitz, Chem. Phys. Lett. **242**, 249 (1995).
[24] J. Laskin, T. Peres, A. Khong, H. A. Jiménez-Vázquez, R. J. Cross, M. Saunders, D. S. Bethune, M. S. de Vries, and C. Lifshitz, Int. J. Mass Spectrom. **185–187**, 61 (1999).
[25] A. Lassesson, K. Mehlig, A. Gromov, A. Taninaka, H. Shinohara, and E. E. Campbell, J. Chem. Phys. **117**, 9811 (2002).
[26] A. Lassesson, A. Gromov, K. Mehlig, A. Taninaka, H. Shinohara, and E. E. B. Campbell, J. Chem. Phys. **119**, 5591 (2003).
[27] A. Lassesson, K. Hansen, M. Jönsson, A. Gromov, E. E. B. Campbell, M. Boyle, D. Pop, C. P. Schulz, I. V. Hertel, A. Taninaka *et al.*, Eur. Phys. J. D **34**, 205 (2005).
[28] S. Suzuki, Y. Kojima, H. Shiromaru, Y. Achiba, T. Wakabayashi, R. Tellgmann, E. E. B. Campbell, and I. V. Herte, Z. Phys. D **40**, 410 (1997).
[29] H. Xiong, R. Obaid, L. Fang, C. Bomme, N. G. Kling, U. Ablikim, V. Petrovic, C. E. Liekhus-Schmaltz, H. Li, R. C. Bilodeau *et al.*, Phys. Rev. A **96**, 033408 (2017).
[30] Z. D. Pešic, D. Rolles, M. Perri, R. C. Bilodeau, G. D. Ackerman, B. S. Rude, A. L. D. Kilcoyne, J. D. Bozek, and N. Berrah, J. Electron. Spectrosc. Relat. Phenom. **155**, 155 (2007).
[31] Z. D. Pešić, D. Rolles, I. Dumitriu, and N. Berrah, Phys. Rev. A **82**, 013401 (2010).
[32] S. M. Hankin, D. M. Villeneuve, P. B. Corkum, and D. M. Rayner, Phys. Rev. A **64** (2001).
[33] M. H. K. Tchaplyguine, O. Dühr, H. Hohmann, G. Korn, H. W. M. H. I. V. Rottke, and E. E. B. Campbell, J. Chem. Phys. **112**, 2781 (2000).
[34] E. E. Campbell, K. Hansen, M. Heden, M. Kjellberg, and A. V. Bulgakov, Photochem. Photobiol. Sci. **5**, 1183 (2006).
[35] P. Scheier, B. Dünser, R. Wörgötter, D. Muigg, S. Matt, O. Echt, M. Foltin, and T. D. Märk, Phys. Rev. Lett. **77**, 2654 (1996).
[36] M. Foltin, O. Echt, P. Scheier, B. Dünser, R. Wörgötter, D. Muigg, S. Matt, and T. D. Märk, J. Chem. Phys. **107**, 6246 (1997).
[37] I. Lamparth, B. Nuber, G. Schick, A. Skiebe, T. Grösser, and A. Hirsch, Angew. Chem. Int. Ed. Engl. **34**, 2257 (1995).
[38] M. J. Van Stipdonk, E. A. Schweikert, and M. A. Park, J. Mass Spectrom. **32**, 1151 (1997).
[39] O. Kornilov, M. Eckstein, M. Rosenblatt, C. P. Schulz, K. Motomura, A. Rouzée, J. Klei, L. Foucar, M. Siano, A. Lübcke *et al.*, J. Phys. B **46**, 164028 (2013).
[40] L. J. Frasinski, V. Zhaunerchyk, M. Mucke, R. J. Squibb, M. Siano, J. H. D. Eland, P. Linusson, P. v.d. Meulen, P. Salén, R. D. Thomas *et al.*, Phys. Rev. Lett. **111**, 073002 (2013).
[41] V. Zhaunerchyk, M. Mucke, P. Salén, P. v. Meulen, M. Kaminska, R. J. Squibb, L. J. Frasinski, M. Siano, J. H. D. Eland, P. Linusson *et al.*, J. Phys. B **46**, 164034 (2013).

[42] S. Cheng, H. G. Berry, R. W. Dunford, H. Esbensen, D. S. Gemmell, E. P. Kanter, T. LeBrun, and W. Bauer, Phys. Rev. A **54**, 3182 (1996).
[43] E. E. B. Campbell, T. Raz, and R. D. Levine, Chem. Phys. Lett. **253**, 261 (1996).
[44] M. Boyle, T. Laarmann, I. Shchatsinin, C. P. Schulz, and I. V. Hertel, J. Chem. Phys. **122**, 181103 (2005).
[45] H. Tang, H. Li, Y. Dou, and W. Fang, Mol. Simul. **36**, 986 (2010).
[46] H. Tang, H. Li, and Y. Dou, Int. J. Mol. Sci. **12**, 353 (2011).
[47] S. G. Kim and D. Tománek, Phys. Rev. Lett. **72**, 2418 (1994).
[48] T. Laarmann, I. Shchatsinin, A. Stalmashonak, M. Boyle, N. Zhavoronkov, J. Handt, R. Schmidt, C. P. Schulz, and I. V. Hertel, Phys. Rev. Lett. **98**, 058302 (2007).
[49] C. E. Klots, Z. Phys. D **21**, 335 (1991).
[50] M.-A. Lebeault, B. Baguenard, B. Concina, F. Calvo, B. Climen, F. Lépine, and C. Bordas, J. Chem. Phys. **137**, 054312 (2012).
[51] K. Gluch, S. Matt-Leubner, O. Echt, R. Deng, J. U. Andersen, P. Scheier, and T. D. Märk, Chem. Phys. Lett. **385**, 449 (2004).
[52] B. Manil, L. Maunoury, J. Jensen, H. Cederquist, H. T. Schmidt, H. Zettergren, P. Hvelplund, S. Tomita, and B. A. Huber, Nucl. Instrum. Methods Phys. Res., Sect. B **235**, 419 (2005).
[53] B. Cao, T. Peres, C. Lifshitz, R. J. Cross, and M. Saunders, Chem. Eur. J. **12**, 2213 (2006).
[54] S. Matt, O. Echt, M. Sonderegger, R. David, P. Scheier, J. Laskin, C. Lifshitz, and T. D. Märk, Chem. Phys. Lett. **303**, 379 (1999).
[55] J. Laskin and C. Lifshitz, J. Mass Spectrom. **36**, 459 (2001).
[56] H. Zettergren, H. T. Schmidt, P. Reinhed, H. Cederquist, J. Jensen, P. Hvelplund, S. Tomita, B. Manil, J. Rangama, and B. A. Huber, Phys. Rev. A **75**, 051201 (2007).
[57] H. Zettergren, H. T. Schmidt, P. Reinhed, H. Cederquist, J. Jensen, P. Hvelplund, S. Tomita, B. Manil, J. Rangama, and B. A. Huber, J. Chem. Phys. **126**, 224303 (2007).
[58] A. A. Agarkov, V. A. Galichin, S. V. Drozdov, D. Y. Dubov, and A. A. Vostrikov, Eur. Phys. J. D **9**, 331 (1999).
[59] Y. J. Lee, N. W. Song, and S. K. Kim, J. Phys. Chem. A **106**, 5582 (2002).
[60] Q. Wang, D. Wu, D. Zhang, M. Jin, F. Liu, H. Liu, Z. Hu, D. Ding, H. Mineo, Y. A. Dyakov *et al.*, J. Phys. Chem. C **113**, 11805 (2009).
[61] T. A. Beu, C. Steinbach, and U. Buck, Eur. Phys. J. D **27**, 223 (2003).